Bonding in metal hexacarbonyls

Ramiro ArratiaPerez and Cary Y. Yang

Citation: The Journal of Chemical Physics **83**, 4005 (1985); doi: 10.1063/1.449115
View online: http://dx.doi.org/10.1063/1.449115
View Table of Contents: http://scitation.aip.org/content/aip/journal/jcp/83/8?ver=pdfcov
Published by the AIP Publishing

Bonding in metal hexacarbonyls

Ramiro Arratia-Perez and Cary Y. Yang
School of Engineering, University of Santa Clara, Santa Clara, California 95053

(Received 8 April 1985; accepted 3 July 1985)

A detailed analysis of the valence molecular orbitals (MO) in $Cr(CO)_6$, $Mo(CO)_6$, and $W(CO)_6$ is presented. A generalized bonding scheme, which includes participation of metal p electrons in the metal–ligand bond, emerges from our results. The metal p electrons are also responsible for effecting mixings between different sets of carbonyl 5σ and 1π orbitals. In these hexacarbonyls, this "σ" + "π" metal–ligand bonding contribution is quantitatively as significant as the well known σ donation and π-back-donation components. The MO's obtained with the Dirac scattered-wave (DSW) method are also used to determine the importance of relativistic effects in this series. The DSW results show that even in $W(CO)_6$, relativistic effects are qualitatively unimportant. Extensive comparisons with existing theoretical and experimental data are made for both ground-state and transition-state calculations.

I. INTRODUCTION

The nature of the metal–ligand bond in carbonyl complexes has been extensively studied in the past two decades.[1–3] The metal carbonyl molecules are sometimes used as model systems for CO chemisorption on metal catalysts,[1–4] and as such, they are thought to share some common bonding characteristics. The current understanding of the electronic structure of terminally bonded metal carbonyls is largely based on two charge transfer mechanisms. First, the so-called CO 5σ donation to metal d orbitals was believed to be the principal mechanism. Then theoretical and experimental data for most carbonyl complexes indicate that significant back-donation from metal d to CO $2\pi^*$ also exists.[5–7] The participation of other orbitals has been recognized[8–13] but detailed quantitative descriptions are lacking.

The metal hexacarbonyl molecules, $M(CO)_6$, M = Cr, Mo, and W, feature two attractive properties which make a detailed investigation of the metal–ligand bond feasible. There is only one metal atom, hence no metal–metal interactions. The carbonyls are octahedrally bonded to the metal atom, resulting in the O_h point group symmetry. Bonding analysis for a high-symmetry system is generally easier. A third attraction for studying this series is that one can follow the effects of relativity down the column of the periodic table from Cr to W, with molecules that are computationally manageable under most molecular orbital (MO) methods.

The purpose of this paper is to present a detailed bonding analysis for the three hexacarbonyls, and to clarify some issues concerning charge transfers between metal and ligands. From this analysis, a complete and generalized description of the metal–ligand bond will emerge. The bonding analysis is based on MO calculations with the self-consistent-$X\alpha$-Dirac-scattered-wave method.[14–16] Comparisons of both ground state and transition state results with existing theoretical and experimental data are made whenever possible. It should be pointed out at the outset that some of the ground state comparisons can only be considered as partial, since all existing data were obtained based on the traditional ($5\sigma \rightarrow d$, $d \rightarrow 2\pi^*$) bonding picture, which we will show to be incomplete.

The organization of this paper is as follows. Section II outlines the calculational procedure. Section III presents the ground state results for all three carbonyls under individual subsections. The generalized bonding scheme is discussed in Sec. IV and transition state results are given in Sec. V.

II. DSW CALCULATIONS

The self-consistent-field-$X\alpha$-Dirac-scattered-wave (DSW) molecular orbital method is a relativistic extension (in the Dirac equation framework) of the nonrelativistic multiple-scattering or scattered-wave technique originally proposed by Slater[17] and subsequently developed by Johnson.[18] The DSW methodology was developed by Yang and coworkers[14–16,19–21] and has been applied to many systems ranging from diatomic molecules to large (20–30 atoms) metal complexes.[15,16,22] Relativistic effects are important in understanding most metal–ligand bonds, especially those involving fourth- or fifth-row transition metals. It has been shown in the clusters $COPt_n$[23,24] that relativistic effects play significant roles in the sd hybridization and metal–molecule bonding. We will attempt to demonstrate in this paper how relativistic effects increase going down the column of the periodic table from Cr to W.

TABLE I. Parameters for DSW calculations, b denotes sphere radii (in bohrs) and α the exchange parameter (from Ref. 33). The interatomic separation d is also given in bohrs.

	$Cr(CO)_6$	$Mo(CO)_6$	$W(CO)_6$
$d_{M\text{-}C}$	3.6282[a]	3.8928[b]	3.9100[c]
$d_{C\text{-}O}$	2.1637	2.1637	2.1900
b_M	2.5763	2.8703	2.8894
b_C	1.4550	1.4550	1.4550
b_O	1.2470	1.2470	1.2470
b_{Out}	7.0389	7.3035	7.3470
α_M	0.7135	0.7034	0.7000
α_C	0.7593	0.7593	0.7593
α_O	0.7445	0.7445	0.7445
$\alpha_{IS} = \alpha_{Out}$	0.7493	0.7350	0.7479

[a] Reference 7.
[b] Reference 32.
[c] Reference 2.

 0021-9606/85/204005-10$02.10

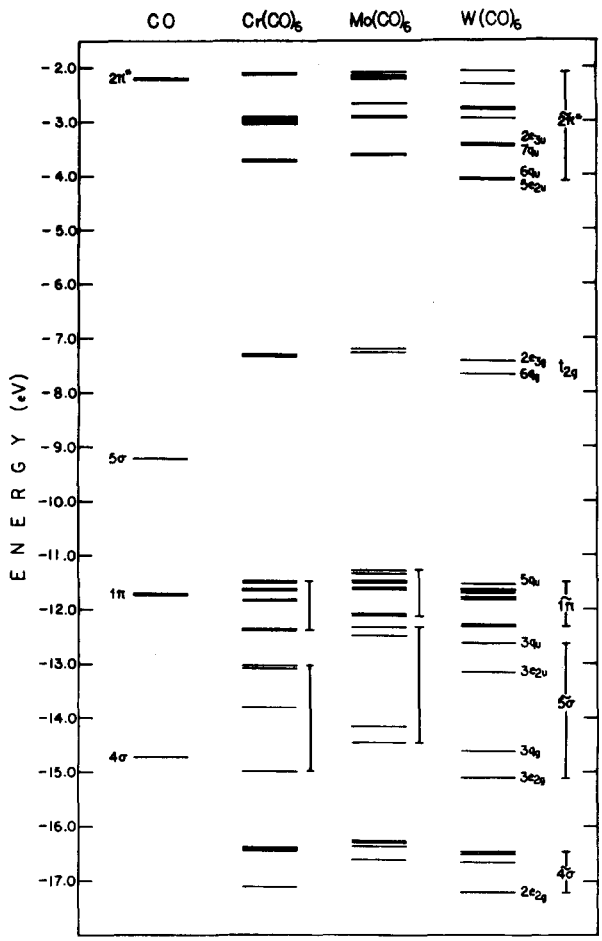

FIG. 1. DSW ground-state valence energy level diagram. $2e_{3g}$ is the HOMO for each carbonyl. The 3σ band is not shown.

The parameters used for the calculations are given in Table I. Two bases were used for each molecule: one "minimal," with partial waves $l \leqslant 4$, $l \leqslant 2$, and $l \leqslant 1$, for the outer, metal, and ligand spheres respectively; the second "extended," with partial waves expansions truncated at $l = 4$ and $l = 2$ for the metal and ligand spheres, respectively. Similar extended basis calculations have been reported in previous nonrelativistic $X\alpha$-SW and Hartree–Fock–Slater-discrete variational method (DVM) calculations on the lighter members of this series.[9–12] Our results using these two bases showed that while the orbital wave functions are not significantly affected going from the minimal to the extended, the ionization energies (IE) generally improve by about 0.5 eV. Thus, to simplify matters, our analyses of ground state results will be based on minimal basis results, while both minimal and extended results will be given for IE's.

The nonrelativistic limit ($C \rightarrow \infty$) was taken for each calculation. As one would expect, relativistic effects become increasingly important going down the column of the periodic table from Cr to W. But as we showed previously,[25] even in $W(CO)_6$, relativistic effects are qualitatively unimportant. In the next section, we will elaborate further on the role of relativity.

Overlapping spheres (10% M–C and 20% C–O) were used as before.[25] The calculational parameters are listed in Table I, and the basis functions for O_h double group symmetry were generated according to the symmetrization scheme described by Yang.[19]

III. GROUND STATE RESULTS

Valence molecular orbital (MO) energies for CO, $Cr(CO)_6$, $Mo(CO)_6$, and $W(CO)_6$ are shown in Fig. 1. Some

TABLE II. Total valence populations for $M(CO)_6$ (units of electrons per atom). NR denotes nonrelativistic SCF-$X\alpha$-DSW ($C \rightarrow \infty$) results.

	$Cr(CO)_6$			$Mo(CO)_6$			$W(CO)_6$		
	NR	DSW		NR	DSW		NR	DSW	
M $s_{1/2}$	0.802	0.812		0.770	0.802		0.778	0.907	
$p_{1/2}$	0.628	0.631		0.618	0.627		0.607	0.642	
	2.00[a]		1.98	2.00		1.97	2.00		1.90
$p_{3/2}$	1.256	1.254		1.237	1.238		1.214	1.220	
Total p	1.884	1.885		1.855	1.865		1.821	1.862	
$d_{3/2}$	2.433	2.442		2.467	2.486		2.460	2.487	
	1.50		1.48	1.50		1.47	1.50		1.40
$d_{5/2}$	3.650	3.622		3.714	3.650		3.691	3.494	
Total d	6.083	6.064		6.190	6.136		6.151	5.981	
Total metal	8.768	8.767		8.815	8.803		8.750	8.750	
C $s_{1/2}$	1.297	1.297		1.300	1.298		1.312	1.298	
$p_{1/2}$	0.767	0.769		0.763	0.767		0.758	0.768	
	2.00		1.99	2.00		1.99	2.00		1.97
$p_{3/2}$	1.534	1.532		1.526	1.525		1.517	1.515	
Total p	2.307	2.301		2.289	2.292		2.275	2.283	
Total carbon	3.598	3.598		3.589	3.590		3.587	3.581	
O $s_{1/2}$	1.551	1.552		1.551	1.551		1.569	1.569	
$p_{1/2}$	1.464	1.466		1.464	1.466		1.462	1.467	
	2.00		1.99	2.00		1.99	2.00		1.99
$p_{3/2}$	2.928	2.925		2.928	2.926		2.924	2.925	
Total p	4.392	4.391		4.392	4.392		4.386	4.392	
Total oxygen	5.943	5.943		5.943	5.943		5.955	5.961	

[a] Ratio of $j = l + \frac{1}{2}$ to $j = l - \frac{1}{2}$ populations.

common features are apparent. For example, the valence complex of each molecule is divided into five subcomplexes or bands, namely, the unoccupied $2\pi^*$, and the occupied t_{2g}, 1π–5σ, 4σ, and 3σ. The characteristics of these bands will be analyzed in detail in the ensuing subsections. In general, the nonrelativistic "t_{2g}" orbital undergoes spin-orbit splitting, ranging from a negligible amount in $Cr(CO)_6$ to almost 0.3 eV in $W(CO)_6$. As we pointed out previously for $W(CO)_6$,[25] relativistic effects tend to stabilize the metal–ligand interactions. Both the nonrelativistic (NR) SCF-$X\alpha$-DSW ($C\rightarrow\infty$) and DSW results given in Table II show a d^6 electron configuration for each molecule with some sp admixtures (2.8 electrons) distributed among the ligand orbitals. The ligands and metal interact through charge transfers among the 4σ, 5σ, 1π, and $2\pi^*$ ligand orbitals, and the metal s, p, and d orbitals. Due to the large volume of data available for the lighter carbonyls, we will analyze the ground state results for each molecule separately.

A. $Cr(CO)_6$

This molecule has been extensively studied, both experimentally[2–4,6,7,29] and theoretically,[8–13] as a model system for transition metal–carbon monoxide bonding, in which the σ donation by the carbonyl is described as being accompanied by $2\pi^*$ back-donation from the metal.[3,7,8–13] The nature of the metal–ligand interaction has been the subject of some controversy among many calculations with varying degrees of sophistication, namely, $X\alpha$-SW[10,12], $X\alpha$-DVM[9,11], *ab initio* Hartree–Fock,[8] restricted Hartree–Fock (RHF),[26] and Fenske–Hall MO.[13] Despite the fact that the Dirac rather than the Schrödinger equation is used, our calculations for $Cr(CO)_6$, which is very much a nonrelativistic system, are basically equivalent to previous $X\alpha$ ones.[9–12] Another consideration in comparing our results with others is how charge distributions are computed under different methods. These distributions may be obtained from projections onto basis sets,[12] from partitioning the intersphere and outer sphere charges among the atoms (as in this study),[27] or from Mulliken population analysis.[8,9,11,13] Hence, charge distributions from these calculations may differ considerably.

Comparing our results with other SW calculations, we note that ours show a rather uniform energy shift with respect to the nonrelativistic results reported by Johnson and Klemperer (JK).[10] Since this molecule is basically nonrelativistic, we attribute this shift to be a result of the different accounting of intersphere charges due to overlapping spheres and slightly different calculational parameters. Another significant difference between ours and JK is the 4σ bandwidth. JK report very little ligand–field splitting for this band while our results show a bandwidth of 0.8 eV. $X\alpha$-DVM calculations,[28] on the other hand, give a bandwidth of 1.5 eV compared with the experimental value of 1.8 eV.[29]

The total valence populations are given in Table II. The small differences between NR and DSW populations can be understood by remembering that in the metal atom, relativistic effects generally lower the s and p orbital energies, but raise the d. Thus, in the molecule, the $4s$ and $4p$ populations of chromium increase by 0.01 and 0.001, respectively, while the $4d$ population decreases by 0.02 electrons. Within the d

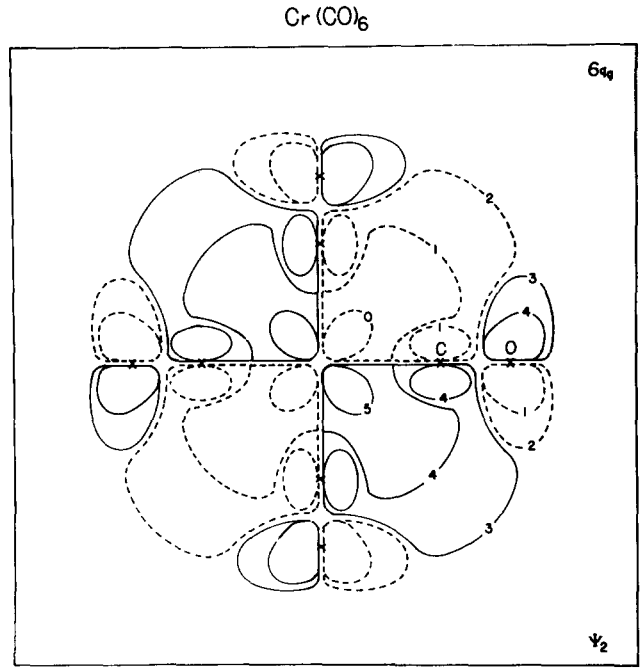

FIG. 2. Contours of the dominant $6q_g$ wave function component of $Cr(CO)_6$ in a plane containing Cr and four sets of ligands CO. Contour values in (electron/bohr^3)$^{1/2}$ are: (0,5), (1,4), (2,3) = ± 0.100, ± 0.010, ± 0.001. These values are the same for all contours presented here. The contour maps for its counterparts in the other two carbonyls are very similar.

populations $d_{3/2}$ orbitals are slightly favored over $d_{5/2}$; the ratio of $l+1/2$ to $l-1/2$ is 1.48 in the DSW calculation, while the NR limit is 1.5. From these ratios given in Table II and the orbital energy diagram, it becomes apparent that relativistic effects in this molecule are negligible, as expected, since Cr is a member of the first transition metal series.

The t_{2g} band consists of a two-fold $2e_{3g}$ and a fourfold $6q_g$. These two orbitals contain primarily metal d character, with some $2\pi^*$ and 1π ligand contributions. They represent a 0.04 eV splitting of t_{2g} due to the small metal $d_{3/2}$–$d_{5/2}$ spin-orbit interaction. From the charge distributions [Table III (A)] for each orbital we observe that the metal contributions in $2e_{3g}$ (65.8%) are purely $d(t_{2g})$, i.e., d_{xz}, d_{yz}, d_{xy}, as required by symmetry, whereas $6q_g$ contains mostly $d(t_{2g})$ and negligible amounts of $d(e_g)$ orbitals ($d_{x^2-y^2}$, d_{z^2}). Both orbitals exhibit similar ligand contributions: 27% $2\pi^*$ and 7% 1π. The ligand π character in this band is clearly shown in the wave function contour map for $6q_g$ (Fig. 2). These charge distributions further confirm that the small splitting of 0.04 eV is due mainly to spin-orbit interactions.

The metal d populations given in Table III (A) are divided into two components. The $d(t_{2g})$ component contains a total of 4.35 electrons distributed mainly among the t_{2g} and 1π bands, while there are a total of 1.72 $d(e_g)$ electrons present mostly in the 5σ and 4σ bands. This $d(e_g)$ character is clearly evident in the wave function contour map for $3q_g$ (Fig. 3). Metal p populations are found primarily in those orbitals originating from the nonrelativistic t_{1u} symmetry, such as $3q_u$ and $3e_{2u}$, where significant 1π–5σ mixing among ligands exists,[7,10] as shown in Table III (A) and illustrated by the wave function contours in Figs. 4 and 5. Both $X\alpha$ papers,[10,28] however, assign these t_{1u} orbitals as primarily from ligand 1π and 5σ. Metal s character is present only

TABLE III. Ground state valence orbital populations(%).

		Cr					$(CO)_6$			
Level	E(eV)	s	p_z	$p_{x,y}$	$d(t_{2g})$	$d(e_g)$	$2\pi^*$	1π	σ	
(A) $Cr(CO)_6$										
$2e_{3u}$	−3.023						99.9	0.1	0.0	
$7q_u$	−3.035			0.0			99.8	0.2	0.0	$2\pi^*$
$6q_u$	−3.707			0.0			85.9	0.2	13.9	
$5e_{2u}$	−3.721		0.0	0.0			87.6	0.8	11.6	
$2e_{3g}$	−7.317				65.8		27.6	6.6	0.0	t_{2g}
$6q_g$	−7.352				66.2	0.0	27.0	6.8	0.0	
$5q_u$	−11.490			6.9			0.2	50.5	42.4	
$4e_{2u}$	−11.509		2.3	4.5			0.2	67.5	25.5	
$5q_g$	−11.639				0.0	0.0	0.1	99.9	0.0	
$4e_{2g}$	−11.658	0.0					0.0	100.0	0.0	1π
$1e_{3u}$	−11.822						5.0	95.0	0.0	
$4q_u$	−11.838			0.0			0.2	81.6	18.2	
$1e_{3g}$	−12.362				6.4		1.3	92.3	0.0	
$4q_g$	−12.377				6.4	0.0	1.3	92.3	0.0	
$3q_u$	−13.041			22.3			0.4	11.0	66.3	
$3e_{2u}$	−13.091		7.5	15.0			0.2	22.2	55.1	5σ
$3q_g$	−13.805				0.0	38.2	0.0	0.0	61.8	
$3e_{2g}$	−14.994	19.4					0.0	0.0	80.6	
$2q_g$	−16.393				0.0	4.6	0.0	0.0	95.4	
$2q_u$	−16.427			2.2			0.0	4.0	93.8	4σ
$2e_{2u}$	−16.431		0.7	1.5			0.0	0.2	97.6	
$2e_{2g}$	−17.105	21.3					0.0	0.0	78.7	
(B) $Mo(CO)_6$										
$2e_{3u}$	−2.930						99.9	0.1	0.0	
$7q_u$	−2.942			0.0			100.0	0.0	0.0	$2\pi^*$
$6q_u$	−3.627			0.4			91.9	0.6	7.1	
$5e_{2u}$	−3.642		0.1	0.3			89.9	0.0	9.7	
$2e_{3g}$	−7.212				64.0		28.3	7.7	0.0	t_{2g}
$6q_g$	−7.288				64.8	0.0	27.1	8.1	0.0	
$5q_u$	−11.295			9.1			0.2	57.0	33.7	
$4e_{2u}$	−11.352		2.6	5.1			0.1	63.0	29.2	
$5q_g$	−11.484				0.0	0.0	0.2	99.8	0.0	
$4e_{2g}$	−11.502	0.0					0.0	100.0	0.0	1π
$1e_{3u}$	−11.618						4.8	95.2	0.0	
$4q_u$	−11.634			0.0			0.0	82.0	18.0	
$1e_{3g}$	−12.092				7.4		1.2	91.4	0.0	
$4q_g$	−12.111				7.5	0.0	1.1	91.4	0.0	
$3q_u$	−12.343			20.3			0.3	15.8	63.6	
$3e_{2u}$	−12.491		7.3	14.7			0.0	26.4	51.6	5σ
$3q_g$	−14.167				0.0	37.7	0.0	0.0	62.3	
$3e_{2g}$	−14.450	26.9					0.0	0.0	73.1	
$2q_u$	−16.258			1.6			0.0	0.0	98.4	
$2e_{2u}$	−16.269		0.6	1.1			0.0	0.0	98.3	4σ
$2q_g$	−16.363				0.0	7.7	0.0	0.0	92.3	
$2e_{2g}$	−16.611	13.2					0.0	0.0	86.8	
(C) $W(CO)_6$										
$2e_{3u}$	−3.438						99.9	0.1	0.0	
$7q_u$	−3.450			0.0			99.8	0.2	0.0	$2\pi^*$
$6q_u$	−4.078			0.5			92.2	0.4	6.9	
$5e_{2u}$	−4.096		0.2	0.3			90.4	0.0	9.1	
$2e_{3g}$	−7.446				58.7		33.2	8.1	0.0	t_{2g}
$6q_g$	−7.675				61.5	0.0	29.5	9.0	0.0	
$5q_u$	−11.535			7.0			0.0	54.5	38.5	
$4e_{2u}$	−11.643		1.3	2.5			0.0	80.1	16.1	
$5q_g$	−11.652				0.0	0.0	0.1	99.9	0.0	
$4e_{2g}$	−11.669	0.0					0.2	99.8	0.0	1π
$1e_{3u}$	−11.784						3.7	96.3	0.0	
$4q_u$	−11.802			0.0			0.1	81.3	18.6	
$1e_{3g}$	−12.280				7.9		1.3	90.8	0.0	
$4q_g$	−12.310				8.5		1.0	90.5	0.0	
$3q_u$	−12.623			21.6			0.5	11.8	66.1	
$3e_{2u}$	−13.156		8.5	17.0			0.2	12.5	61.8	5σ
$3q_g$	−14.607				0.0	34.5	0.0	0.0	65.5	
$3e_{2g}$	−15.101	20.8					0.0	0.0	79.2	
$2q_u$	−16.468			1.9			0.0	0.0	98.1	
$2e_{2u}$	−16.518		0.9	1.9			0.0	0.0	97.2	4σ

TABLE III. (*continued*).

		Cr					$(CO)_6$			
Level	E(eV)	s	p_z	$p_{x,y}$	$d(t_{2g})$	$d(e_g)$	$2\pi^*$	1π	σ	
$2q_g$	−16.667				0.0	11.7	0.0	0.0	88.3	
$2e_{2g}$	−17.210	24.5					0.0	0.0	75.5	
(D)W(CO)$_6$ ($c\rightarrow\infty$)										
$2e_{3u}$							99.9	0.1	0.0	
	−3.423									
$7q_u$				0.0			99.9	0.1	0.0	$2\pi^*$
$6q_u$				0.45			90.9	0.2	8.4	
	−4.061									
$5e_{2u}$			0.15	0.30			90.7	0.3	8.5	
$2e_{3g}$					62.5		28.4	9.1	0.0	t_{2g}
	−7.729									
$6q_g$					62.5	0.0	28.4	9.1	0.0	
$5q_u$				8.4			0.1	58.6	32.9	
	−11.490									
$4e_{2u}$			2.8	5.6			0.1	58.4	33.1	
$5q_g$					0.0	0.0	0.1	99.9	0.0	
	−11.650									
$4e_{2g}$		0.0					0.1	99.9	0.0	1π
$1e_{3u}$							0.1	99.9	0.0	
	−11.787									
$4q_u$			0.0			0.1	99.9	0.0		
$1e_{3g}$					8.7		1.2	90.1	0.0	
	−12.299									
$4q_g$					8.7	0.0	1.1	90.2	0.0	
$3q_u$				20.4			0.0	30.1	49.4	
	12.515									
$3e_{2u}$			6.8	13.6			0.1	30.0	49.5	5σ
$3e_{2g}$	−14.487	25.9					0.0	0.0	74.1	
$3q_g$	−14.615				0.0	34.9	0.0	0.0	65.0	
$2q_u$				1.72			0.0	0.0	98.2	
	−16.429									
$2e_{2u}$			0.57	1.15			0.0	0.0	98.2	4σ
$2q_g$	−16.637				0.0	11.9	0.0	0.0	88.1	
$2e_{2g}$	−16.795	12.9					0.0	0.0	87.1	

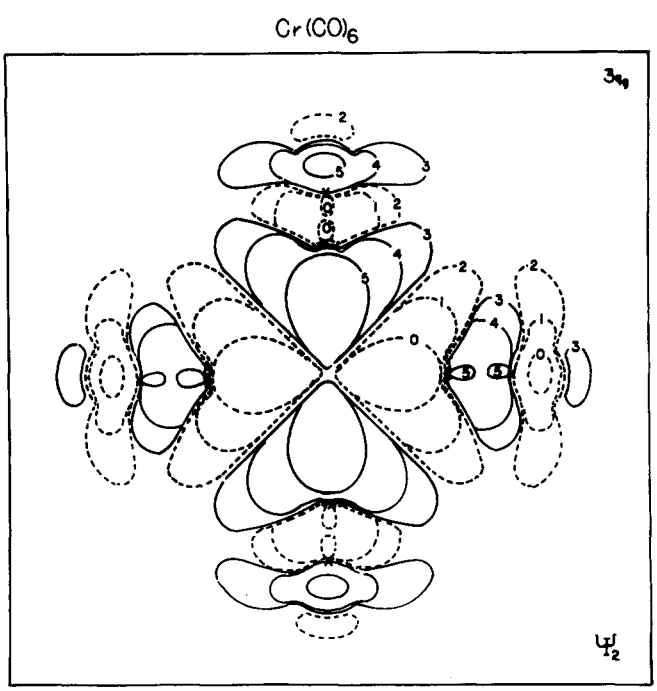

FIG. 3. $3q_g$ of $Cr(CO)_6$.

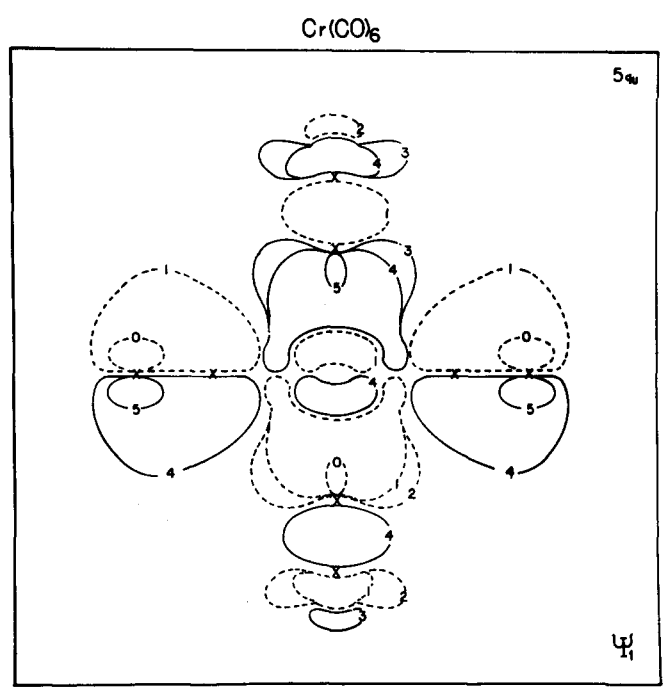

FIG. 4. $5q_u$ of $Cr(CO)_6$.

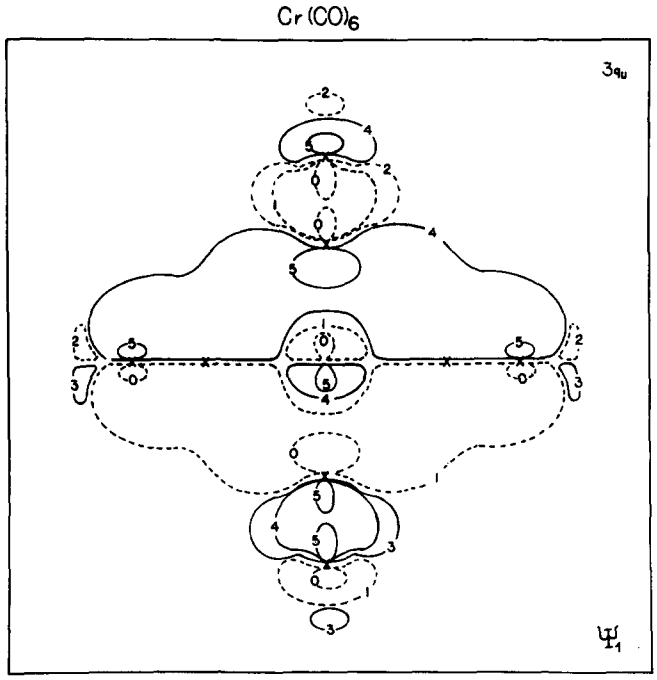

FIG. 5. $3q_u$ of $Cr(CO)_6$.

in the e_{2g} orbital in each of the 5σ and 4σ bands, as dictated by symmetry.

The ligand orbitals of t_{1u} nonrelativistic symmetry are split, largely due to spin-orbit interaction of the $4p_{3/2}$ and $4p_{1/2}$ metal contents, into the twofold degenerate e_{2u} and fourfold degenerate q_u orbitals. In $Cr(CO)_6$, these splittings are all inconsequentially small. The metal–ligand admixtures in these orbitals are probably related to the 5σ–1π mixing. For example, from Table III (A), the $5q_u$ and $4e_{2u}$ orbitals contain 42% and 26% 5σ character, respectively, while their 1π contents are 51% and 67%. The balance consists entirely of metal p character. The total amount of metal $4p$ character in the three t_{1u} orbitals represents a ligand donation to metal of 1.89 electrons, of which 1.34 electrons are donated by the 5σ band, and only 0.41 electron is donated by the 1π. The ligand donation to Cr $4s$ takes place only in the $3e_{2g}$ and $2e_{2g}$ orbitals, and amounts to 0.39 and 0.42, electron, respectively. The amount of charges back-donated by metal $3d$ to the ligands $2\pi^*$ and 1π can also be computed from Table III (A), the result being 1.63 electrons to $2\pi^*$ and 0.40 to 1π. Overall, as summarized in Table IV, the $M\rightarrow L$ back-donation represents a loss of 2.03 electrons by the $3d$ (t_{2g}) orbitals and the $L\rightarrow M$ donation amounts to a gain of 4.80 metal electrons, mostly by $4s$, $4p$, and $3d$ (e_g). This gives rise to a net electron transfer of 2.77 electrons from ligand to metal, or a net loss of 0.46 electron per ligand molecule.

Our analysis of the metal–carbonyl bond so far is based on the DSW orbital populations of the molecule. No approximations or simplifications beyond those inherent in the MO method have been employed. Thus, from the charge transfer summary in Table IV, we can conclude that metal s, p, and d as well as ligand 4σ, 5σ, 1π, and $2\pi^*$ all participate in the metal–ligand bonding. However, in order to compare our results with existing data, we have to keep in mind the simplified description of the metal–carbonyl bond in terms of charge transfers between only metal d and ligand 5σ and $2\pi^*$ orbitals.[7–13] In view of this "partial" bonding picture adopted by others, we present a detailed comparison of some of our orbital populations with existing theoretical and experimental values (Table V). The metal $4s$ and $4p$ contributions are omitted since they are not addressed under this simplified bonding picture. In general, our results compare rather well with others. We hasten to reiterate, however, that the ($d\rightarrow 2\pi^*$, $5\sigma\rightarrow d$) bonding picture is incomplete, as we will discuss in more detail in Sec. IV.

In arriving at the net charge transfer of 0.46 electron per carbonyl from ligand to chromium, we have taken every molecular orbital into account. It would be both difficult and misleading to compare this value with other estimates, 0.2[12], -0.2 to -0.3[11], and zero,[7] which were all obtained with the partial bonding picture.

B. $Mo(CO)_6$

Valence molecular orbital energies for $Mo(CO)_6$ are also shown in Fig. 1. The overall features are similar to those for

TABLE IV. Summary of charge transfers (in electrons).[a]

		$L\rightarrow M$						Net charge transfer $L\rightarrow M$ (electron/CO)
		s	p	d	Total	$M\rightarrow L$		
	$Cr(CO)_6$							
	$1\pi\rightarrow$Cr	0.00	0.41	0.39	0.80	$3d\rightarrow 1\pi$	0.40	
	$5\sigma\rightarrow$Cr	0.39	1.34	1.53	3.26	$3d\rightarrow 2\pi^*$	1.63	
	$4\sigma\rightarrow$Cr	0.42	0.14	0.18	0.74			
	Total:	0.81	1.89	2.10	4.80		2.03	0.46
	$Mo(CO)_6$							
ω	$1\pi\rightarrow$Mo	0.00	0.51	0.45	0.96	$4d\rightarrow 1\pi$	0.48	
	$5\sigma\rightarrow$Mo	0.54	1.25	1.51	3.30	$4d\rightarrow 2\pi^*$	1.65	
	$4\sigma\rightarrow$Mo	0.26	0.10	0.32	0.68			
	Total:	0.80	1.86	2.28	4.94		2.13	0.47
	$W(CO)_6$							
	$1\pi\rightarrow$W	0.00	0.36	0.50	0.86	$5d\rightarrow 1\pi^*$	0.53	
	$5\sigma\rightarrow$W	0.42	1.37	1.38	3.17	$5d\rightarrow 2\pi^*$	1.84	
	$4\sigma\rightarrow$W	0.49	0.13	0.47	1.09			
	Total:	0.91	1.86	2.35	5.12		2.37	0.46

[a] 3σ ligand donations are negligible.

TABLE V. Orbital population comparisons for $Cr(CO)_6$.

	DSW	HF[a]	$X\alpha$-DVM[b]	$X\alpha$-SW[c]	FH-MO[d]	Expt[e]
CO-5σ	1.78	...	1.69	...	1.52	1.60
CO-2π^*	0.32	...	0.48	...	0.52	0.40
Cr-3d (e_g)	1.71	0.75	1.28	1.32	...	1.2,1.5[f]
Cr-3d (t_{2g})	4.35	3.31	3.37	4.44	...	3.8,4.5[f]
d ($e_{g/d}$(%)	28	18	28	23	...	25 ± 3

[a] Reference 8.
[b] Reference 9.
[c] Reference 12.
[d] Reference 13.
[e] Reference 7.
[f] Reference 7, with $3d^5 4s^1$ and $3d^6$ Cr configuration.

$Cr(CO)_6$. Nonrelativistic and relativistic (DSW) valence populations are given in Table II. The Mo atom in the molecule contains 8.80 valence electrons, resulting in a net gain of 0.47 electron from each ligand molecule. Relativistic effects are still insignificant, as evidenced by the $(l + 1/2)/(l - 1/2)$ ratios and the small t_{2g} spin-orbit splitting (0.08 eV). This small splitting has introduced difficulties in interpreting the vibronic levels originating from the $2E''$ and $2U'$ states.[6]

From the detailed population analysis given in Table III (B), we find that in the 1π band there are 0.51 electron and 0.45 electron donated from the ligands to the Mo 5p and 4d orbitals respectively. The latter donation constitutes the d (t_{2g}) contribution to the 1π band, as in $Cr(CO)_6$. Since there is no metal s character in the 1π band, the total ligand donation to the metal in this band amounts to 0.96 electron. The 5σ band shows ligand donations to the 5s, 5p, and 4d metal orbitals of 0.54, 1.25, and 1.51 electrons, respectively. As in $Cr(CO)_6$, the 4d population in 5σ consists almost entirely of metal d (e_g), with negligible d (t_{2g}) contamination. The ligand donations from the 4σ band to the 5s, 5p, and 4d metal orbitals are 0.26, 0.10, and 0.32 electron, respectively, which are considerably less than those from 5σ. For $M \rightarrow L$, we find that there are 1.65 and 0.48 electrons back-donated from the metal to the $2\pi^*$ and 1π ligand orbitals, respectively. To summarize, the total $L \rightarrow M$ donations add up to 4.94 electrons, while the $M \rightarrow L$ back-donation amounts to 2.13 electrons. Hence, as we point out earlier, a net transfer of 0.47 electron from each ligand molecule results. The total metal d population consists of 30% d (e_g) and 70% d (t_{2g}), compared with the corresponding values of 28% and 72% in $Cr(CO)_6$.

The 4σ bandwidth of 0.4 eV is only half of its counterpart in $Cr(CO)_6$, as it contains considerably less metal s character. The situation in the 5σ band is different, however, since both bandwidths (~ 2 eV) and metal contents are similar in the two molecules. Small relativistic effects are evident in the 0.15 eV spin-orbit splitting of $3t_{1u}$ into $3q_u$ and $3e_{2u}$. As in $Cr(CO)_6$, the spin-orbit splitting originates from the metal p character contained in these two orbitals. The large separation between this t_{1u} complex and the other two orbitals within the 5σ band is probably due to increased 1π–5σ hybridization in $3t_{1u}$.

C. $W(CO)_6$

Since the general features of the valence electronic structure of this molecule (see Fig. 1) were discussed in a previous communication,[25] we will focus here on a comparative study of $W(CO)_6$ with its lighter counterparts. As we have demonstrated previously,[25] the relativistic effects in this molecule, which is the heaviest of the three carbonyls, are qualitatively unimportant. From the preceding discussion, we see that $Cr(CO)_6$ is clearly a nonrelativistic system, while relativistic effects in $Mo(CO)_6$ are far from being quantitatively significant. In $W(CO)_6$, although measurable spin-orbit splittings exist,[6,29] the general nature of the metal–ligand bond could be correctly described using a purely nonrelativistic treatment.

Since W is the heaviest metal atom of the three, the t_{2g} (HOMO) spin-orbit splitting (~ 0.3 eV) in this carbonyl is the largest. Also the $(l + 1/2)/(l - 1/2)$ ratios shown in Table II deviate more from their NR limits. From the orbital populations given in Table III (C), we note that as in the other two carbonyls the 1π band contains the smallest amount of metal character, while the 5σ, 4σ, and t_{2g} bands show significant metal contribution from the 6s, 6p, and 5d W orbitals. The computed total ligand donation from 1π to W is 0.86 electron, of which 0.36 electron is transferred to 6p. The remaining charge goes to 5d. Similar to the other carbonyls, the metal–ligand interactions are most pronounced in the 5σ complex, where metal s, p, and d orbitals are all present. In particular, the total ligand donation to W from 5σ amounts to 3.17 electrons, of which 1.37 electrons are donated to 6p, 1.38 electrons to 5d, and 0.42 electron to 6s. A unique feature of this 5σ band is the 0.53 eV separation of $3q_u$ and $3e_{2u}$. This splitting is mainly a result of the $6p_{3/2}$–$6p_{1/2}$ spin-orbit interaction, which is considerable for W. This large splitting, combined with the 5σ–1π hybridization present in these two orbitals, effectively widens the 5σ bandwidth to about 2.5 eV, which is almost 0.5 eV larger than those in the lighter carbonyls. The 4σ bandwidth is about 0.8 eV, a consequence of both ligand field effects and the relativistic stabilization of the $2e_{2g}$ orbital, which contains 25% W 6s character. The total ligand donation from this band amounts to 1.09 electrons.

Again, similar to the others, the $M \rightarrow L$ back-donation takes place in the t_{2g} band. The back-donated charges to the $2\pi^*$ and 1π ligand orbitals are 1.84 and 0.53 electron, respectively, giving rise to a total back-donation of 2.37 electrons. If we add up the charges donated from 1π, 5σ, and 4σ, we obtain a total $L \rightarrow M$ donation of 5.12 electrons. Hence, the net charge transfer is again $L \rightarrow M$, with 0.46 electron per

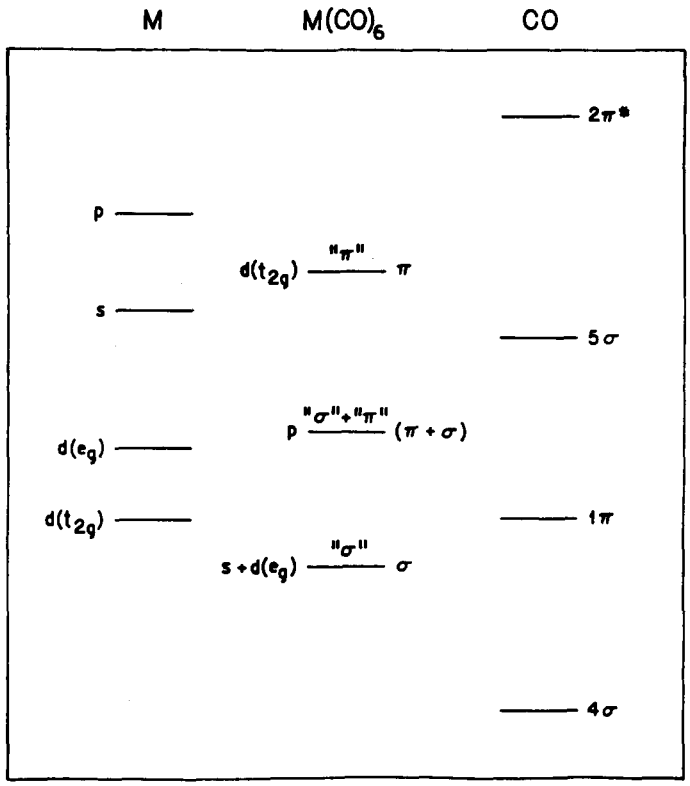

FIG. 6. Representation of general bonding scheme for metal hexacarbonyls.

ligand molecule. As one can see in Table IV, this result is almost invariant for all three carbonyls.

IV. GENERAL BONDING PICTURE

An interesting consequence of the octahedral symmetry of these molecules is that there is a clear grouping pattern of σ and π M–C and C–O bonds. This pattern is illustrated in a schematic diagram shown in Fig. 6. There are essentially three types of metal–ligand bonds, each of which was analyzed separately in the preceding paragraphs. First, the $d(t_{2g})$ + COπ bond is formed largely as a result of $2\pi^*$ back-donation. This is a π *metal–ligand* bond as clearly shown in the $6q_g$ contour map (Fig. 2). The second bond is one that involves hybridization of σ and π and, at least for these molecules, is shown to be equally important as the others.[30] This bond is made up of three t_{1u} orbitals, namely, $(5q_u, 4e_{2u})$, $(3q_u, 3e_{2u})$, and $(2q_u, 2e_{2u})$. From the contour maps for $5q_u$ and $3q_u$ (Figs. 4 and 5), and the population analysis, we conclude that this bond is formed by mixing σ orbitals of one set of carbonyls ("longitudinal") with π orbitals of another set ("transverse") through p orbitals of the metal. The longitudinal (parallel to p) metal–ligand bond is σ, while the transverse is π. Hence, we denote this p + CO$(\sigma + \pi)$ bond by $\sigma + \pi$. We also note that the $5q_u$ orbital (Fig. 4) shows 1π–5σ ligand–ligand antibonding character, whereas $3q_u$ (Fig. 5) contains 1π–5σ ligand–ligand bonding contributions. The third metal–ligand bonding type is the well known σ donation, resulting obviously in a σ metal–ligand bond (Fig. 3).

There are two issues surrounding the exact roles played by each of these three bonding types. The first concerns which orbitals within the valence complex (excluding 3σ) exhibit these bonding characteristics. The answer to this can be determined partly from symmetry considerations and partly from population analysis. Single-group symmetry requires that the π type could be present in any t_{2g} orbitals, the σ in e_g and a_{1g}, and the $\sigma + \pi$ in t_{1u}. Thus, for this class of molecules, we can find π in t_{2g} and 1π bands, σ in 5σ and 4σ, and $\sigma + \pi$ in 1π, 5σ, and 4σ. For $Cr(CO)_6$ (and the other two as well), π is found mainly in t_{2g}, with a small contribution from $1e_{3g}$ and $4q_g$ in 1π [Tables III (A)–III(C)]. However, this 1π contribution, which consists of donation to $d(t_{2g})$ by almost the same amount backdonated by $d(t_{2g})$ to 1π, effectively brings about an almost purely $2\pi^*$ back-donation metal–ligand π bond. The σ bond is present in the $q_g(e_g)$ and $e_{2g}(a_{1g})$ orbitals of 5σ and 4σ, whereas $\sigma + \pi$ manifests itself in three t_{1u} orbitals as discussed above. While double-group considerations alter this pattern somewhat, a close comparison between Tables III (C) and III (D) reveals that even for $W(CO)_6$, the charge transfer between metal and ligand is not substantially affected by relativity. In fact, the major redistribution of charges due to relativistic effects occur only among ligands, in the form of different 1π–5σ mixings in q_u and e_{2u} orbitals within the 1π–5σ complex. Thus the single-group picture we subscribe to is essentially accurate for these molecules.

The second issue focuses on the relative importance of each bonding type. While the existence of an exact quantitative representation is debatable, the extent of each bonding type can be characterized qualitatively as follows. The role of the π bond largely depends on the amount of $2\pi^*$ back-donation. The importance of $\sigma + \pi$ bond is most probably enhanced by increased ligand donation to the metal p orbitals. The amount of charge transferred from ligand to metal $d(e_g)$ and s must increase with stronger σ metal–ligand bond. For $Cr(CO)_6$, where $2\pi^*$ back-donation amounts to 1.63 electrons, donation to metal p 1.89, and donation to metal $d(e_g)$ and s 2.53, all three types are unquestionably present. In fact, one can conclude that $2\pi^*$ back-donation plays a significant role in the metal–ligand bonding, and it might also be an important factor in the C–O bond weakening as observed in IR and Raman spectra.[31]

V. TRANSITION-STATE RESULTS

One way of testing the quality of wave functions determined by a MO method is to compute molecular properties from them and compare with available experimental data. A substantial collection of experimental information exists for these metal hexacarbonyls, such as, UV and x-ray photoelectron spectra[2,6,29] and UV optical absorption measurements.[3,34] Table VI summarizes results of spin-restricted transition state[17] calculations for the ionization energies (IE) and for the two symmetry allowed $d \rightarrow CO(2\pi^*)$ charge-transfer excitations. Calculated IE's for both minimal and extended basis sets are included. The use of f and g polarization functions for each metal, and d functions for the ligands, yields uniformly better comparisons with experimental IE's by about 0.5 eV.

As we pointed out earlier, the spin-orbit splitting of the

TABLE VI. Ionization and transition energies (eV). Results for both minimum and extended basis sets are presented.

Transition	Minimum	Extended	Other calculations	Experiment
(A) $Cr(CO)_6$				
$2e_{3g} \rightarrow$vacuum	9.86	9.47	8.60[a], 9.80[b], 8.90[c]	8.50[f]
$6q_g \rightarrow$vacuum	9.90	9.51	8.80,8.30[d], 10.70[e]	8.40[g]
$2e_{3g} \rightarrow 6q_u$	3.82	...	3.90[a]	4.44[h]
$6q_g \rightarrow 7q_u$	4.53	...	4.80[a]	5.48[h]
(B) $Mo(CO)_6$				
$2e_{3g} \rightarrow$vacuum	9.66	9.13		8.50[g]
			8.80[k]	8.45[f]
$6q_g \rightarrow$vacuum	9.74	9.21		8.40[i]
$2e_{3g} \rightarrow 6q_u$	3.80	...	3.95[j]	4.32[h,j]
			4.14[k]	
$6q_g \rightarrow 7q_u$	4.55	...	4.53[j]	5.44[h]
				5.41[j]
(C) $W(CO)_6$				
$2e_{3g} \rightarrow$vacuum	9.84	9.35		8.30,[g] 8.33[f]
$6q_g \rightarrow$vacuum	10.10	9.60		8.56,[g] 8.59[f]
$2e_{3g} \rightarrow 6q_u$	3.54	...		4.30[h]
$6q_g \rightarrow 7q_u$	4.42	...		4.83[h]

[a] Reference 10.
[b] Reference 26.
[c] Reference 28.
[d] Reference 11.
[e] Reference 8.
[f] Reference 6.
[g] Reference 29.
[h] Reference 3.
[i] Reference 2.
[j] Reference 34.
[k] Reference 35.

t_{2g} band into $2e_{3g}$ and $6q_g$ increases from $Cr(CO)_6$ to $W(CO)_6$, the values being 0.04, 0.08, and 0.25 eV, respectively. The small splittings in $Cr(CO)_6$ and $Mo(CO)_6$ might complicate the interpretation of vibrational fine structure.[6] The splitting in $W(CO)_6$ has been well characterized,[6,29] and our calculated values of 0.26 eV (minimum basis) and 0.25 eV (extended basis) compare well with the experimental value of 0.26 eV.[6,29]

The results of other nonrelativistic calculations for $Cr(CO)_6$ are also given in Table VI (A). In general, we observe that transition state calculations [10,11,28] give better results that those that utilize Koopman's theorem.[8,26] Our DSW results for IE's are about 1 eV larger than their experimental counterparts. The IE reported by JK[10] is the closest to experiment. This agreement is probably an accident resulting from the unphysical "negative" interphere probability density due to overlapping spheres. The more accurate $X\alpha$-DVM,[9,11,28] which has no space-partitioning requirements, yields rather good comparisons with experiment. While our DSW transition state results fare less well than DVM, due mainly to the space-partitioning approximation in the scattered-wave theory, they are obtained with substantially less computational effort. Moreover, little additional costs are required to extend the calculations to each of the heavier carbonyls. Thus, the DSW method, though quantitatively less accurate, is more versatile and practical for the development and elucidation of detailed bonding trends and relativistic effects down the column or across the row of the periodic table.

Finally, results of transition state calculations, obtained using minimal basis sets, for the lowest $d \rightarrow CO(2\pi^*)$ transitions are also given in Table VI. The allowed transitions are compared with experimental UV optical absorption results.[3,34] The differences (between $\sim$0.4 eV and 1 eV) are similar to those for the IE's. We attribute this discrepancy to the spin-restricted transition state calculations and correlation effects that are not well represented by this local density functional method. Furthermore, the space-partitioning approximation in the realm of the scattered-wave formalism poses the usual problem,[15,16,22] and it generally affects the outermost valence and unoccupied orbitals more. This problem is somewhat alleviated by the semiempirical approach of choosing overlapping sphere radii, but the extent of this "correction" is very difficult to assess.

VI. CONCLUSIONS

The calculations presented here represent the first detailed comparative study of an isoelectronic series of molecules using the DSW method. The results have yielded two major findings. First, they confirm a generalized description of the bonding in these molecules. Metal p electrons not only play a significant role in the metal–ligand bond, but they also bring about important mixings between different sets of carbonyl 5σ and 1π orbitals. This $\sigma + \pi$ metal–ligand bond has been previously ignored in consideration of metal–carbonyl bonding in molecules and in CO chemisorption systems. The second finding provides a definitive answer to the often-raised question of how important are relativistic effects in

these molecules. From our results with the three metal carbonyls, Cr to W down the column of the periodic table, we have concluded that relativistic effects are qualitatively unimportant for the valence orbitals even in $W(CO)_6$.[25] Since the DSW method treats relativistic effects fully in the one-electron local density framework,[16] it poses little difficulty in identifying them for each molecule.

While the method has demonstrated its remarkable ability in establishing bonding trends and elucidating relativistic effects, one must not lose sight of its inherent limitations. As we pointed out in comparing the DSW transition state results with other calculations and with experiments, the local density approximation and the space-partitioning scheme contained in the method generally result in some degree of quantitative inaccuracies. Further, the use of the spin-restricted procedure in transition state calculations may introduce additional correlation-related errors. In order to account for correlation effects in the DSW framework, a configuration interaction approach has recently been proposed.[36]

Further work on metal carbonyls is in progress. The study involves DSW calculations on fifth-row transition metal carbonyls,[37] from which we hope to understand the bonding trend going across this row of the periodic table. Finally, we believe that the two major findings summarized above are method independent, though the detailed numbers may differ from one method to another. For example, recently reported nonrelativistic results on $Ni(CO)_4$ using other techniques[38,39] showed large populations of metal $4p$, though these two cited papers disagree on the extent of the metal $4p$ participation in the metal–ligand bonding. In the hexacarbonyls considered here, the metal p electrons represent the keys in bringing about mixings between longitudinal σ and transverse π carbonyl orbitals giving rise to the $\sigma + \pi$ bond. While CO ($\sigma + \pi$) mixings are not disallowed by symmetry in $Ni(CO)_4$, its geometry suggests that the role of the metal p orbitals in effecting such mixings is probably less significant. Since the understanding of metal carbonyl bonding serves as a precursor to gaining insight into the much more complex situation in CO chemisorption,[30] the tools as well as the approach used here seem to be suitable for the latter.

ACKNOWLEDGMENTS

We wish to thank David Case for many useful discussions. This work was supported by the U.S. Department of Energy, Division of Chemical Sciences, through Contract No. DE-AC03-82ER13011.

[1] E. Muetterties, Chem. Rev. **79**, 91 (1979).
[2] E. W. Plummer, W. R. Salaneck, and J. S. Miller, Phys. Rev. B **18**, 1673 (1978); G. Loubriel and E. W. Plummer, Chem. Phys. Lett. **64**, 234 (1979).
[3] N. A. Beach and H. B. Gray, J. Am. Chem. Soc. **90**, 5713 (1968).
[4] D. R. Lloyd, C. M. Quin, and N. V. Richardson, Solid State Commun. **20**, 409 (1976).
[5] F. A. Cotton and G. Wilkinson, *Advanced Inorganic Chemistry*, 3rd ed. (Wiley–Interscience, New York, 1972).
[6] J. L. Hubbard and D. L. Lichtenberger, J. Am. Chem. Soc. **104**, 2132 (1982).
[7] B. Rees and A. Mitschler, J. Am. Chem. Soc. **98**, 7918 (1976).
[8] I. H. Hillier and V. R. Saunders, Mol. Phys. **22**, 1025 (1971).
[9] W. Heiser, E. J. Baerends, and P. Ros, J. Mol. Struct. **63**, 109 (1980).
[10] J. B. Johnson and W. G. Klemperer, J. Am. Chem. Soc. **99**, 7132 (1977).
[11] E. J. Baerends and P. Ros, Mol. Phys. **30**, 1735 (1975).
[12] B. E. Bursten, D. G. Freier, and R. F. Fenske, Inorg. Chem. **19**, 1810 (1980); K. G. Caulton and R. F. Fenske, *ibid.* **7**, 1273 (1968).
[13] D. E. Sherwood and M. B. Hall, Inorg. Chem. **19**, 1805 (1980); L. W. Yarbrough and M. B. Hall, *ibid.* **17**, 2269 (1978).
[14] C. Y. Yang and S. Rabii, Phys. Rev. A **12**, 362 (1975).
[15] C. Y. Yang, *Relativistic Effects in Atoms, Molecules and Solids*, edited by G. Malli (Plenum, New York, 1983), p. 335.
[16] C. Y. Yang and D. A. Case, *Local Density Approximations in Quantum Chemistry and Solid State Physics*, edited by J. Dahl and J. P. Avery (Plenum, New York, 1984), pp. 643–664.
[17] J. C. Slater, Adv. Quantum Chem. **6**, 1 (1972); J. Chem. Phys. **43**, 5228 (1965).
[18] K. H. Johnson, Adv. Quantum Chem. **7**, 143 (1973); Annu. Rev. Phys. Chem. **26**, 39 (1975).
[19] C. Y. Yang, J. Chem. Phys. **68**, 2626 (1978).
[20] D. A. Case and C. Y. Yang, Int. J. Quantum Chem. **18**, 1091 (1980).
[21] D. A. Case and C. Y. Yang, J. Chem. Phys. **72**, 3443 (1980).
[22] D. A. Case, Annu. Rev. Phys. Chem. **33**, 151 (1982).
[23] C. Y. Yang and D. A. Case, Surf. Sci. **106**, 523 (1981).
[24] C. Y. Yang, H. L. Yu, and D. A. Case, Chem. Phys. Lett. **81**, 170 (1981).
[25] C. Y. Yang, R. Arratia-Perez, and J. P. Lopez, Chem. Phys. Lett. **107**, 112 (1984).
[26] L. G. Vanquickenborne and J. Velhurst, J. Am. Chem. Soc. **105**, 1769 (1983).
[27] D. A. Case and M. Karplus, Chem. Phys. Lett. **39**, 33 (1976); R. Arratia-Perez and D. A. Case, J. Chem. Phys. **79**, 4939 (1983).
[28] E. J. Baerends and P. Ros, Int. J. Quantum Chem. Symp. **12**, 169 (1978).
[29] B. R. Higginson, D. R. Lloyd, P. Burroughs, D. M. Gibson, and A. F. Orchard, J. Chem. Soc. Faraday Trans. 2 **69**, 1659 (1973).
[30] F. Greuter, D. Heskett, E. W. Plummer, and H. J. Freund, Phys. Rev. B **27**, 7117 (1983).
[31] L. H. Jones, R. S. McDowell, and M. J. Goldblat, J. Chem. Phys. **48**, 2663 (1968).
[32] M. Hargittai and I. Hargittai, *The Molecular Geometries of Coordination Compounds in the Vapour Phase* (Elsevier, New York, 1977), p. 187.
[33] K. Schwarz, Phys. Rev. B **5**, 2466 (1972); Theor. Chim. Acta **34**, 225 (1974).
[34] W. C. Trogler, S. R. Desjardins, and E. I. Solomon, Inorg. Chem. **18**, 2131 (1979).
[35] J. C. Giordan, J. H. Moore, and J. A. Tossell, J. Am. Chem. Soc. **103**, 6632 (1981).
[36] D. A. Case, Chem. Phys. Lett. **109**, 66 (1984).
[37] R. Arratia-Perez, C. Y. Yang, and J. P. Lopez (to be published).
[38] C. W. Bauschlicher, Jr. and P. S. Bagus, J. Chem. Phys. **81**, 5889 (1984).
[39] D. Spangler, J. J. Wendoloski, M. Dupuis, M. M. L. Chen, and H. F. Schaefer, J. Am. Chem. Soc. **103**, 3985 (1981).